A CYCLIC TRACKING PROCEDURE FOR COLLISION PROBABILITY CALCULATIONS IN 2-D LATTICES

R. Roy, G. Marleau, A. Hébert and D. Rozon
Groupe d'Analyse Nucléaire
Institut de Génie Énergétique, École Polytechnique de Montréal
Montréal (Québec), Canada H3C 3A7

ABSTRACT

The integral transport equation with isotropic scattering and sources is solved in general 2-D Cartesian geometries in the case where specular boundary conditions are taken into account. First, using selected angular directions, a cyclic tracking procedure is set up in order to follow the infinite path of neutrons in a regular 2-D lattice. Collision probability (CP) calculations are then performed by summing closed-form contributions resulting from the infinite line integration on these cyclic tracks. Numerical comparisons with benchmark solutions are presented in order to show the overall accuracy of this method. Extensions to the case of anisotropic scattering are also discussed.

1. INTRODUCTION

The exact representation of complex lattices (composed of mixed cylindrical-rectangular or cylindrical-hexagonal geometries) is important in transport calculations. This goal can be achieved using the integral form of the transport equation often discretized via first-flight region-to-region collision probabilities (CP), which are then used to solve lattice problems in the case of isotropic scattering and sources.[1] After a decomposition of the domain into homogeneous regions, a tracking routine is used to compute the intersections of the trajectories with the different homogeneous regions in the domain; CPs are then computed by combining the track lengths obtained from the tracking routine with the total cross sections in the domain. Generally, CP methods have restricted the treatment of boundary conditions to an isotropic reflection on the overall external surface of the domain. This approximation, known as "white" boundary conditions, was found to be useful for cylindrical cell models.[2] A better approach is to impose specular boundary conditions in the true geometry of the cell (or the group of cells), in order to take into account the exact neutron behaviour on each surface of the domain. The only perfect way

to account for specular boundary conditions is to follow the neutron path on the whole infinite domain which is a lattice of the original reflected cell repeated with a coherent mirror-like rotation-inversion process. This can be approximatively done by tracking the neutron path past the external boundaries, assuming that the original domain is extended to cover the whole space. The attenuation of neutrons at each surface can then be considered and the tracking routine proceeds until the neutrons have traveled a fixed optical distance (say 10 mean free paths) after which contributions are neglected. In order to perform such a tracking in multigroup calculations, knowledge of the physical properties of the geometry is necessary. An adequate tracking file may be difficult to obtain if we introduce void regions or, even simply, if we vary some cross sections (with burnup for example) in the domain.

Another alternative consists of selecting a numerical quadrature which imposes the tracks to be "cyclic" in the sense that a track finishes where it has started after a finite number of crossings of the cell under investigation. Such a tracking was successfully implemented in the code CACTUS,[3] which uses the method of characteristics to solve the transport equation. The cyclic tracking has two advantages: 1) only a finite number of track lengths is required to represent infinite tracking, 2) there is no *a priori* need to truncate a line as a function of the physical properties of the regions crossed. Once the tracking has been performed, one can still integrate approximatively the CPs using truncated lines. However, there is also the option of explicitely integrating the infinite lines as in reference 4. This formalism was developed as a component of the EXCELL module in the DRAGON transport code.[5] In this paper, the objectives are mainly the validation of the cyclic tracking procedure and the ability to use this procedure to perform benchmark calculations using the infinite tracking-line integration; no attempt was done to vectorize or to minimize computing costs yet.

In section 2, we will describe how we select the basic 2-D angle sets that are compatible with the cyclic tracking procedure and how we compute weights associated with these angles. Section 3 presents details on the infinite line integration that has to be performed when computing CP contributions of a cyclic track. In section 5, we will compare our results with those of other authors for some 2-D standard test problems. Finally, we will describe future work on anisotropy, 3-D rectangular lattices and draw some conclusions.

2. GENERATING CYCLIC TRACKS

Consider the basic domain of a 2-D Cartesian lattice and assume that specular boundary conditions are associated with the external surfaces. This basic domain is first partitioned into I homogeneous regions and is extended to fill up the whole space using specular replication. Assuming that the neutron angular direction Ω is described by $\mu = \cos\theta$ where θ is the polar angle measured from the z-axis, and by ϕ the azimuthal angle measured from the x-axis, we define the following symmetric CP from region i to region j:

$$P_{ij} = \int_0^{2\pi} \frac{d\phi}{2\pi} \int_{\perp\phi} dr' \zeta_{ij}(\phi, r') \int_0^1 \frac{d\mu}{\sqrt{1-\mu^2}} F_{ij}(\phi, r', \mu) \tag{1}$$

where dr' stands for an element of the line perpendicular to the angle ϕ. A 2-D track, determined by (ϕ, r'), will intersect a certain number of regions in the lattice. The characteristic function $\zeta_{ij}(\phi, r')$ is either 1 if this track intersects region i before region j in direction ϕ or 0 otherwise. For a particular track, the factors $F_{ij}(\phi, r', \mu)$ collect the contributions from all segments $[s_i, s_{i+1}]$ of region i to all segments $[s_j, s_{j+1}]$ of region j and are given by line integrals of the form:

$$\int_{s_i}^{s_{i+1}} ds \int_{s_j}^{s_{j+1}} ds' \beta_{ij} \exp[-|\Sigma_i^\mu (s_{i+1} - s) + T_{i+1}^\mu - T_j^\mu - \Sigma_j^\mu (s_j - s')|] \tag{2}$$

where Σ_j^μ is the total cross section for region number j divided by $\sqrt{1-\mu^2}$ and where T_j^μ and β_{ij} are respectively the optical path from $s' = 0$ to $s' = s_j$ (the 3-D optical path) and the total albedo attenuation from $s = s_{i+1}$ to $s' = s_j$. Should the μ-integration of equation (1) be performed, the regular formulation of 2-D CPs using Bickley functions is obtained.[1] In that case however, the multiplicative property of the exponential function is lost and the boundary conditions must be approximated to some extent using isotropic surface currents. One alternative is to carry out the μ-integration numerically rather than analytically and to circumvent the use of a series of Bickley function evaluations.

The next step is now to describe the numerical integration of equation (1) in the variables (ϕ, r'). Here, a cyclic tracking procedure can be used in such a way that a grid of tracks (straight lines) are arranged so that each track ends at its own starting point. This basic idea is already used in the characteristics formulation of the transport equation,[3] but the CP formulation is somewhat different. To perform CP integrations, the user specifies two values: a prime number p that will be used to generate the angles and an approximative density d, in tracks/cm, that is required for track separation. Let us now concentrate on the angular quadrature scheme. In a basic domain of dimensions $X \times Y$, we define a set of angles in $[0, \pi/2]$ given by:

$$\phi_k = \tan^{-1} \frac{kY}{(p-k)X}, \qquad k = 0, 1 \ldots p.$$

The ϕ-integration of equation (1) is done using these angular coordinates associated with a set of positive weights that are calculated in order to preserve even moments of the neutron flux. The angles 0 and $\pi/2$ were kept because it was found that, with these two points, weights were regularly increasing up to $\pi/4$. The density d is automatically adjusted for every angle to obtain the nearest possible density required by an equally spaced track separation, and is used for the r'-integration.

The choice to take a prime number can be understood by the fact that it provides some knowledge concerning the tracking path in the domain. Except possibly for the angles 0 and $\pi/2$, a cyclic track in the ϕ_k direction will cross the basic domain $2(p-k)$

times in the $x-$direction and $2k$ times in the $y-$direction before returning to its starting point (see Figure 1). The track period is thus defined by $\mathcal{L}_k = 2\sqrt{\{(p-k)X\}^2 + \{kY\}^2}$, so that increasing the number of angles will result in an increase of the track periods. Once generated by this procedure, the tracking file is used to numerically compute volumes for every angle, and all track lengths are renormalized angle by angle in order to preserve the true volume of all regions of the geometry.

Note that the μ-integration is performed using a Gauss-Legendre quadrature in the interval $[0,1]$ with an order of accuracy compatible with the ϕ-integration.[6] Another interesting possibility, not studied here, would be to use an equal-weight Gauss-Chebyshev quadrature which is compatible with the form of the last integration in equation (1). However, this is true only for isotropic scattering and, in order to provide an adequate frame for extensions to the case of anisotropic scattering, the choice was made to use a $(p+1)/2$ simple Gauss-Legendre quadrature for the μ-integration associated with a given prime number p. Table 1 gives an example of the angular parameters obtained for the cyclic tracking of a square domain with $p = 11$ and $d = 20$. These particular parameters will be used in section 4 in order to present some numerical results.

This cyclic tracking procedure can be generalized to other user-defined sets of points and weights; in CACTUS for example, one tracking option is to select ideal points and weights which are then adequately modified in order to generate cyclic tracks.[3] The cyclic tracking procedure being given, we will examine how these tracks can be used to perform CP calculations.

3. INFINITE LINE INTEGRATION ALONG CYCLIC TRACKS

The key point of the integration process is that all the contributions to F_{ij} must be added *prior* to performing the final μ-integration. Consider a cyclic track of period $\mathcal{L}$ decomposed into K successive segments

$$T = \{(N_k, L_k);\ k = 1 \text{ to } K\}$$

where N_k represents the region number and L_k is the length of the segment. We will now summarize the infinite line integration on the particular cyclic track T. The first step is to replace the infinite integration by a finite one. This is done by summing the contribution of each period weighted by a factor $\beta_{tot}e^{-\tau_{tot}}$ which accounts for neutron source attenuation after each period; this sum is performed analytically and leads to an infinite cycle multiplication factor:

$$\alpha^{\infty} = (1 - \beta_{tot}e^{-\tau_{tot}})^{-1} \quad \text{with} \quad \tau_{tot} = \sum_{k=1}^{K} \Sigma^{\mu}_{N_k} L_k.$$

Since the track may cross regions i and j more than once in a period, one must be careful to add all the contributions of the form (2). The resulting expression for F_{ij} is:

$$F_{ij} = \sum_{k=1}^{K}\sum_{l=1}^{K} \delta_{iN_k}\delta_{jN_l}[\delta_{kl}d_k + \alpha^{\infty}c_k c_l \beta_{kl}e^{-\tau_{kl}}] \tag{3}$$

where δ is the usual Kronecker delta function and where τ_{kl} and β_{kl} are now the optical path and the total albedo attenuation over a cycle from the end of region k to the beginning of region l (hence $\beta_{kk} = \beta_{tot}$ and $\tau_{kk} = \tau_{tot} - \Sigma^{\mu}_{N_k} L_k$). The c_k-factors are defined by:

$$c_k = \int_0^{L_k} ds\, e^{-\Sigma_i^{\mu} s} = \begin{cases} \dfrac{1 - e^{-\Sigma^{\mu}_{N_k} L_k}}{\Sigma^{\mu}_{N_k}} & \text{if } \Sigma^{\mu}_{N_k} \neq 0 \\ L_k & \text{if } \Sigma^{\mu}_{N_k} = 0. \end{cases}$$

Contributions from a line segment to itself are treated separately using the d_k-factors defined by:

$$d_k = \frac{1}{2} \int_0^{L_k} ds \int_0^{L_k} ds'\, e^{-\Sigma_i^{\mu} |s - s'|} = \begin{cases} \dfrac{L_k - c_k}{\Sigma^{\mu}_{N_k}} & \text{if } \Sigma^{\mu}_{N_k} \neq 0 \\ \frac{1}{2} L_k^2 & \text{if } \Sigma^{\mu}_{N_k} = 0. \end{cases}$$

It is clear from equation (3) that the reciprocity relation $F_{ij} = F_{ji}$ can be used to simplify the calculation of symmetric CPs. These factors are similar to the ones already presented for slab geometries,[4] the only significant difference is that all total cross sections are here divided by $\sqrt{1 - \mu^2}$ instead of μ; they can also be coherently used in void regions. Once all the F_{ij} factors of equation (3) have been computed, one may proceed to region-to-region CP numerical integration of equation (1). For a domain decomposed into I regions, the original transport problem is now converted into the following system of linear equations:

$$V_j \varphi_j = \sum_{i=1}^{I} P_{ij} \{ \Sigma_{si} \varphi_i + q_i \} \tag{4}$$

where V_j and φ_j are the volume and the mean flux in region j and where Σ_{si} and q_i are the scattering cross section and the sources in region i. The linear equations in (4) are simply solved by direct inversion of the scattering contributions, leading to the scattering modified collision probabilities.

We now give some remarks on the extension of the cyclic tracking procedure to the anisotropic case. In this case, we use a spherical harmonic expansion of the angular sources inside every homogeneous region and we integrate the source contributions from region i giving collisions in region j. The anisotropic CP formulation is similar to the one described above with the added difficulty that the angular mode may change for a given track when crossing an external surface due to the parity properties of the spherical harmonics. All the contributions corresponding to a given angular mode associated with specific values of the expansion functions must be added before performing CP reconstruction.[4] We will now study some numerical results obtained by this procedure in the isotropic case.

4. NUMERICAL RESULTS

The new cyclic tracking procedure described above was integrated in the CP module EXCELL, part of the DRAGON lattice code. In order to show the precision of the cyclic tracking procedure, we will present some well-known one-group test problems. All tests were performed on an IBM ES-9000 computer with single precision arithmetics except for CP double precision accumulators; results are compared to various other computing methods (Monte Carlo, finite element or other CP methods). We investigated four square lattice problems with homogeneous rectangular subdivisions and a 7×7 PWR assembly with mixed cylindrical-rectangular geometry. Unless explicitly stated, all dimensions in theses problems are given in cm and all cross sections are in cm^{-1}; the input track density d are in tracks/cm. The four external faces are labeled X_-, X_+, Y_- and Y_+, and these respectively refer to lines $y = 0$, $y = y_{\max}$, $x = 0$ and $x = x_{\max}$.

4.1 Slab Half Thickness Eigenvalue Problem

The first problem is intended to show the coherence of the 2-D results obtained by the cyclic tracking procedure as compared to equivalent one-dimensional results. The problem is a 2-D mock-up of a slab eigenvalue problem, and was investigated for various 2-D angular quadratures in reference 6. The geometry for this eigenvalue problem is a pure-absorber homogeneous square region of 1 mfp side with one vacuum and three reflective boundaries; fission was represented here by a uniform value of $\nu\Sigma_f = 1$. This domain is subdivided into 4, 8, 16, 32 and 64 equivolumetric slices parallel to the vacuum boundary. The cyclic tracking procedure was performed for these splittings using $p = 7, 11$ and 19 and increasing track densities $d = 4, 8, 16, 32$ and 64 respectively. Comparative results were obtained for an equivalent 1-D slab domain where the CP computation is done using the same Gauss points as for the μ–integration in the 2-D domain as described in section 2. Five-significant-figure accuracy was requested for the flux, and the results of Table 2 are exhibited to six digits. Since the region splittings and the parameters of the μ–integration are equivalent for the 1-D and 2-D problems, these results exhibit the errors generated by the (ϕ, r') integration in equation (1) and it is easily seen that the two last columns of the table are almost identical because of the greater number of angles chosen.

4.2 Lathrop Source Problem

We will now study the standard one-group Lathrop test case.[6,7] The geometry of this problem is a square $[0,2] \times [0,2]$ domain with a unit source located in $[0,1] \times [0,1]$; the total and scattering cross sections throughout the domain are respectively $\Sigma_t = 0.75$ and $\Sigma_s = 0.5$. Reflective boundaries are present on the two faces X_- and Y_-, and vacuum boundaries on X_+ and Y_+. Using the cyclic tracking parameters $p = 11$ and $d = 20$ tracks/cm, we performed CP calculations with various mesh decompositions. Comparisons using semi-analytic formulas for the CPs have shown that the maximum error on fluxes is less than 0.15% for the 2×2 and 4×4 equally space mesh intervals in this problem. Table 3 gives percentages of particles escaping the system, as compared with the S_{16} 30×30 result given in reference 7. The right edge flux of a 16×16 result

for tracking parameters $p = 11$ and $d = 40$ is also given in Figure 2; as one can see, very little flux oscillation remains even with only 12 azimuthal angles.

4.3 Watanabe-Maynard Void Problem

We will now study a standard void problem with fixed sources.[8,9] The ability to treat void problems is one of the important features of the cyclic tracking procedure. In this source problem, a square source region is surrounded by a void followed by a scattering region. The geometry of the problem is shown in Figure 3 together with DRAGON data input. The WAT8, WAT16 and WAT24 geometries are similar except that the number of equivolumetric regions are respectively 64, 256 and 576. The tracking parameters are respectively $p = 11$ and $d = 4, 8, 12$.

In Table 4, flux values are given in the top right-hand corner of the domain and compared to the results obtained by the MCNP Monte Carlo code and the FELTRAN finite element code as given in reference 9. The WAT8 fluxes are directly taken from the output flux map, but the WAT16 fluxes have been linearly interpolated over four surrounding regions. There is an excellent overall agreement between the MCNP and the cyclic tracking solutions. In Figure 4, we give flux values obtained for the three geometries along the line $X = 5.625$ cm. One can see that the WAT24 flux has a little bump around $Y = 4.0$ cm; this bump is not produced by ray effect distortion and a similar behaviour was found in other computations.[8]

4.4 Tsai-Loyalka Problem

This problem, set by Tsai and Loyalka,[10] is similar to the Lathrop problem except that three boundaries are now perflectly reflectives. An infinite set of square-in-square cells arranged in line network are physically represented by this problem. The geometry of this problem is a square $[0,1] \times [0,1]$ domain with a spatially constant source in $[0,0.52] \times [0,0.52]$; all these dimensions are given in mfp's and the isotropic source is fixed to 1 n cm^{-3} s^{-1}. Reflective boundaries are present on the three faces X_-, Y_- and Y_+, and there is one vacuum boundary on X_+. The problem was run using various scattering cross sections respectively given using the number of secondaries by $c = \Sigma_s/\Sigma_t = 1.00, 0.50, 0.10, 0.05$ and 0.00. The domain was split using 25×25 equivolumetric regions.

The EXCELL module was run using $p = 7, 11$ and 19, with input density $d = 100.0$. The integral and S_{16} solutions were taken from reference 10. When looking at the results given in Table 5, one must be aware that the three last columns represent mean flux values over regions centered at the selected points $x = y = 0.50, 0.70, 0.98$ whereas the point fluxes at the same coordinates were obtained from the integral solution. The main differences occurring at $x = y = 0.5$ mfp can be explained by a stronger flux gradient at that point. In Figure 5, we show the relative errors on flux values obtained with angular parameters $p = 7$ and 11 as compared to reference flux of the $p = 19$ solution along the line $X = 0.5$ mfp; this comparison is useful to see the stability of the method when keeping the density fixed and modifying the number of angles. We can see that the $p = 11$ fluxes on this line are within 2% of the $p = 19$ solution.

4.5 PWR 7 × 7 Assembly

Our last test case represents a small PWR assembly with a central burnable poison rod. This test was set by Stankovski[11] and used to compare various 2-D CP approximations. All cells in this assembly have two material regions, a 0.45 cm radial region containing fuel (except for the central cell which contains poison), surrounded by a 1.25 cm pitch moderator region; fixed sources are assumed in the moderator region. There is no leakage in this problem and specular reflections are applied on all external faces of the 7 × 7 assembly; Figure 6 depicts the cell numbering used in one-eight of the assembly together with DRAGON geometric and material input.

Reference values were obtained from MARSYAS direct CP calculations where tracking is done over the whole infinite domain with truncated tracks as explained in the introduction section. The treatment of boundary conditions is therefore accurate, and the only difference is the selected angles which are regular for MARSYAS and irregular for the cyclic tracking procedure in EXCELL. Tracking parameters $p = 11$ and $d = 8.0$ were used here. As seen in Table 6, the MARSYAS and EXCELL results are very close; the maximum relative error is in moderator region of cell number 1, where the smallest absorption rate can be found, but note that the absolute discrepancy remains very small.

5. DISCUSSION

One-group numerical results have shown that it is possible to use the cyclic tracking procedure to obtain accurate solutions to the integral transport equation in its isotropic formulation. Extension of the method is already developed and partly coded for anisotropic scattering problems of any order, and results will be presented later on that subject. The most important features of the cyclic tracking procedure are that no approximation is made to include the boundary conditions and that it can easily be applied to void problems; moreover, no ray effect (flux oscillations) have been found in testing our cyclic tracking procedure. For middle size problems (not too optically large domains split into not more than a few hundred regions), we conclude that this integral method is accurate. As a new option of the module EXCELL, part of the Canadian DRAGON lattice code, the code development described above will provide adequate integral solutions for standard lattices. The flux maps obtained can then be coherently used to condense and homogenize cross sections and to define diffusion coefficients, as part of the whole reactor chain calculations.

To complete the procedure, further work and tests are necessary to see the effect of 2-D cyclic angular quadratures on rectangular (non-square) lattices. In order to provide a global deterministic package, development of a 3-D capability is the next step; this development will be done with the same idea of using the directional tracking and keeping the angular integration of the CPs to the end. It is not impossible to use the same idea for hexagonal cells or lattices, at least for the isotropic scattering option; the main problem here would be to correctly formulate the boundary conditions. Finally, in order to apply the procedure in a production environment, vectorization of the CP integration process would also be necessary.

Acknowledgements—This work has been carried out with the aid of a grant from Hydro-Québec, for which we wish to express our appreciation.

REFERENCES

[1] R. SANCHEZ and N. J. McCORMICK, *Nucl. Sci. Eng.*, **80**, 481 (1982).

[2] R. J. J. STAMM'LER and M. J. ABBATE, "Methods of Steady-State Reactor Physics in Nuclear Design," Academic Press, London (1983).

[3] M. J. HALSALL, "CACTUS, A Characteristics Solution to the Neutron Transport Equation in Complicated Geometries," Report AEEW-R 1291, Atomic Energy Establishment, Winfrith (1980).

[4] R. ROY, *Ann. nucl. Energy*, **17**, 379 (1990).

[5] G. MARLEAU, A. HÉBERT and R. ROY, "DRAGON: A Collision Probability Transport Code for Cell and Multicell Calculations," Report IGE-100, École Polytechnique de Montréal (1990).

[6] I. K. ABU-SHUMAYS, *Nucl. Sci. Eng.*, **64**, 299 (1977).

[7] K. L. LATHROP, *Nucl. Sci. Eng.*, **45**, 255 (1971).

[8] Y. WATANABE and C. W. MAYNARD, "The Discrete Cones Method in Two Dimensional Neutron Transport Computations," Report UWFDM-574, University of Wisconsin (1984).

[9] R. T. ACKROYD and N. S. RIYAIT, *Ann. nucl. Energy*, **16**, 1 (1989).

[10] R. W. TSAI and S. K. LOYALKA, *Nucl. Sci. Eng.*, **61**, 536 (1976).

[11] Ž. STANKOVSKI, *Nucl. Sci. Eng.*, **92**, 255 (1986); see also A. KAVENOKY, M. LAM-HIME and Ž. STANKOVSKI, "Improvements of the Integral Transport Theory Method," *Proc. Topl. Mtg. Computational Methods in Nuclear Engineering*, Williamsburg, Virginia, April 23–25, 1979, Vol. 2, p. 7-55 (1979).

Table 1. Points and Weights Obtained from Cyclic Tracking in a Square Domain for Angular Parameters $p = 11$, $d = 20$.

k	direction $\cos\phi_k$	weight w_k	density d_k
0	1.000000	0.029932	20.000000
1	0.995037	0.069253	20.099751
2	0.976187	0.082326	18.439089
3	0.936329	0.095964	21.360009
4	0.868243	0.107722	20.155644
5	0.768221	0.114804	19.525624
6	0.640184	0.114804	19.525624
7	0.496139	0.107722	20.155644
8	0.351123	0.095964	21.360009
9	0.216930	0.082326	18.439089
10	0.099504	0.069253	20.099751
11	0.000000	0.029932	20.000000

Table 2. Eigenvalues for the Slab Half Thickness Problem as Function of Spatial Discretization and Angular Quadrature.

# of mesh subdivisions	2-D tracking $p = 7$	1-D slab equivalent[a]	2-D tracking $p = 11$	1-D slab equivalent	2-D tracking $p = 19$	1-D slab equivalent
4	0.780734	0.780707	0.780815	0.780785	0.780802	0.780790
8	0.782292	0.782379	0.782417	0.782402	0.782418	0.782412
16	0.782708	0.782849	0.782852	0.782859	0.782866	0.782861
32	0.782814	0.782971	0.782964	0.782980	0.782980	0.782980
64	0.782840	0.783001	0.782992	0.783011	0.783009	0.783010
Exact	0.783024					

[a] 1-D results obtained with same Gauss points used in 2-D tracking

Table 3. Percent Escapes and CPU Times for the Lathrop Problem.

Splitting	*escape*	CPU
2 × 2	41.69%	0.5 s
4 × 4	40.56%	1.0 s
8 × 8	40.22%	4.4 s
16 × 16	40.12%	47.9 s
S_{16} 30 × 30	40.11%	

Table 4. Flux Values in the Top Right-hand Corner of the Watanabe-Maynard Problem.

	Split [option]	X=5.625 cm	X=6.875 cm	X=8.125 cm	X=9.375 cm
Y=5.625 cm	WAT8	2.3099	1.7783	1.3441	0.9087
	WAT16	2.3133	1.7879	1.3441	0.9095
	[Feltran Ext.]	2.3451	1.7779	1.3191	0.9105
	[MCNP]	2.3114	1.7563	1.3273	0.9242
Y=6.875 cm	WAT8	1.7783	1.5043	1.1332	0.8020
	WAT16	1.7879	1.5125	1.1356	0.7999
	[Feltran Ext.]	1.7779	1.4762	1.1343	0.7917
	[MCNP]	1.7929	1.4938	1.1290	0.7925
Y=8.125 cm	WAT8	1.3441	1.1332	0.9204	0.6600
	WAT16	1.3441	1.1356	0.9231	0.6587
	[Feltran Ext.]	1.3191	1.1343	0.9042	0.6428
	[MCNP]	1.3323	1.1564	0.9033	0.6426
Y=9.375 cm	WAT8	0.9087	0.8020	0.6600	0.4821
	WAT16	0.9095	0.7999	0.6587	0.4795
	[Feltran Ext.]	0.9105	0.7717	0.6428	0.4643
	[MCNP]	0.9208	0.8038	0.6606	0.4869

Table 5. Flux Values for Selected Points in the Tsai-Loyalka Problem.

$x = y$	integral solution	S_{16} solution	$p = 7$ EXCELL	$p = 11$ EXCELL	$p = 19$ EXCELL
c = 1.00					
0.50	1.17403	1.15225	1.16208	1.15951	1.15755
0.70	0.81085	0.80384	0.80001	0.80063	0.80056
0.98	0.50290	0.48985	0.50119	0.49816	0.49671
c = 0.50					
0.50	0.42728	0.41046	0.42792	0.42452	0.42268
0.70	0.21309	0.21186	0.21271	0.21301	0.21286
0.98	0.12864	0.12606	0.12876	0.12819	0.12814
c = 0.10					
0.50	0.28859	0.27303	0.29072	0.28736	0.28558
0.70	0.11644	0.11468	0.11572	0.11623	0.11609
0.98	0.06882	0.06796	0.06869	0.06861	0.06876
c = 0.05					
0.50	0.27764	0.26222	0.27988	0.27654	0.27476
0.70	0.10926	0.10748	0.10856	0.10910	0.10895
0.98	0.06447	0.06372	0.06432	0.06427	0.06443
c = 0.00					
0.50	0.26755	0.25224	0.26990	0.26657	0.26480
0.70	0.10273	0.10094	0.10206	0.10262	0.10247
0.98	0.06050	0.05983	0.06034	0.06033	0.06050

Table 6. Absorbtion Rates for Pin and Moderator Regions in Cells of the PWR Assembly.

Cell #	Region	MARSYAS	EXCELL	Relative error[a]
1	pin	0.83799	0.83752	−0.056%
	moderator	0.00689	0.00681	−1.134%
2	pin	0.73979	0.73820	−0.215%
	moderator	0.03571	0.03573	+0.062%
3	pin	0.82218	0.82474	+0.311%
	moderator	0.03991	0.03993	+0.056%
4	pin	0.85166	0.85140	−0.031%
	moderator	0.04104	0.04096	−0.199%
5	pin	0.78722	0.79197	+0.603%
	moderator	0.03824	0.03825	+0.026%
6	pin	1.67049	1.67388	+0.203%
	moderator	0.08092	0.08081	−0.131%
7	pin	1.71199	1.70780	−0.245%
	moderator	0.08252	0.08228	−0.296%
8	pin	0.85350	0.85276	−0.087%
	moderator	0.04120	0.04103	−0.410%
9	pin	1.72122	1.71667	−0.264%
	moderator	0.08328	0.08276	−0.625%
10	pin	0.86023	0.86246	+0.259%
	moderator	0.04174	0.04139	−0.831%

[a] MARSYAS results serve as reference values in the error calculation.

Figure 1. Example of a Cyclic Track ($X = Y$ and $p = 3, k = 2$).

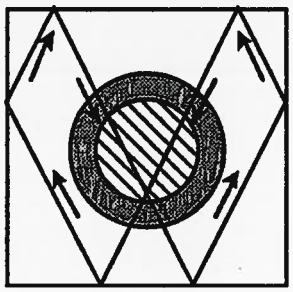

Figure 2. Flux at $x = 1.9375$ cm for the 16 × 16 Splitting.

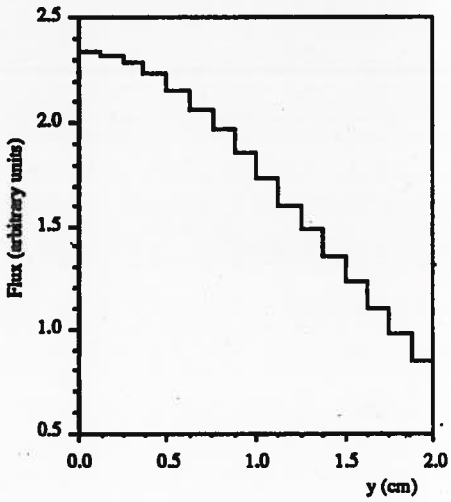

Figure 3. Geometry of the Watanabe and Maynard's Problem with DRAGON Input.

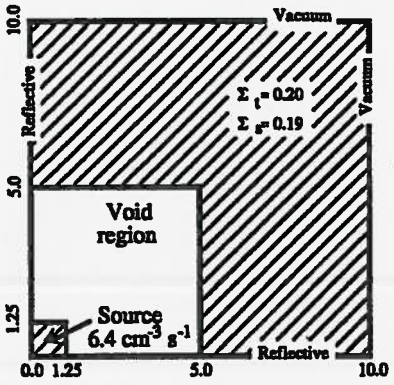


```
$MAC ;
 READ INPUT
 MIX 1 TOTAL 0.2 SCAT 1 1 0.19 FIXE 6.4
 MIX 2 TOTAL 0.2 SCAT 1 1 0.19
 MIX 3 TOTAL 0.0 SCAT 1 1 0.00
 STOP
$GEO ;
 WAT8 :- CAR2D 3 3
                MIX 1    3    2
                    3    3    2
                    2    2    2 ;
 X- REFL MESHX 0.00 1.25 5.00 10.00 X+ VOID
          SPLITX   1    3    4
 Y- REFL MESHY 0.00 1.25 5.00 10.00 Y+ VOID
          SPLITY   1    3    4
 ENDG
 WAT16 :- WAT8
          SPLITX   2    6    8
          SPLITY   2    6    8
 ENDG
 WAT24 :- WAT8
          SPLITX   3    9   12
          SPLITY   3    9   12
 ENDG
 STOP
```

Figure 4. Flux along $X = 5.625$ cm in the Watanabe and Maynard's Problem.

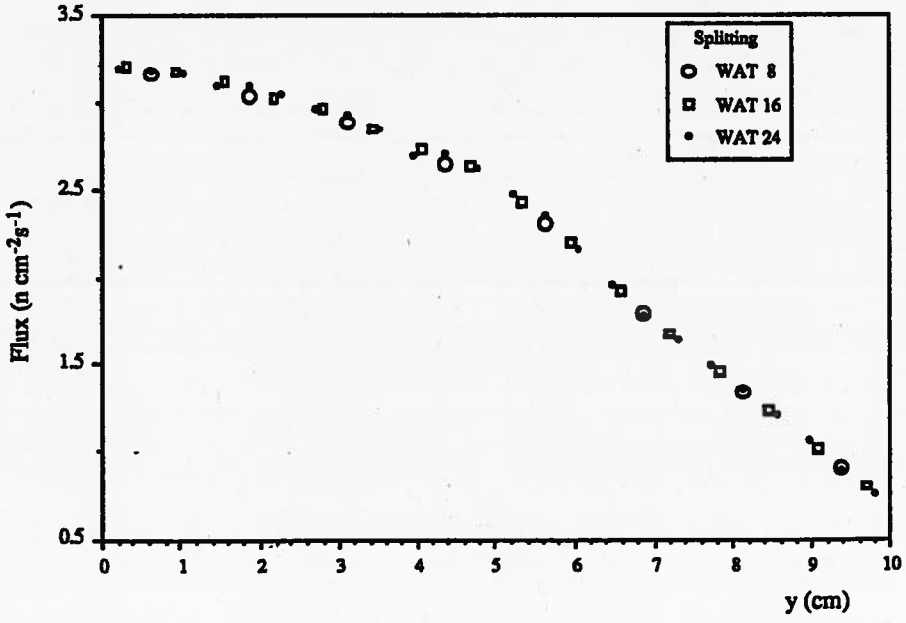

Figure 5. Relative flux errors in Tsai-Loyalka problem for $c = 0.0$ along line $X = 0.5$ mfp. Flux values obtained for $p = 7$ and 11 are compared to $p = 19$ reference values.

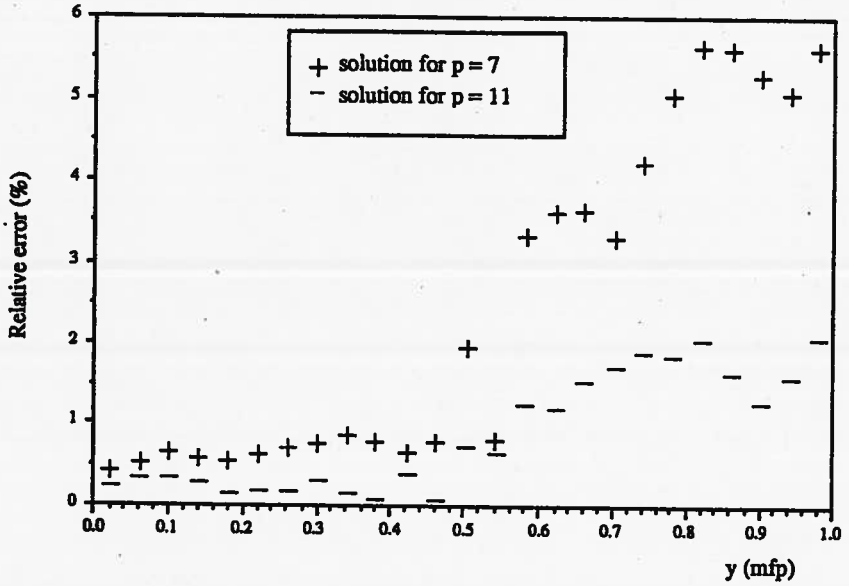

Figure 6. Geometry of the MARSYAS Problem with Cell Numbering and DRAGON Input.

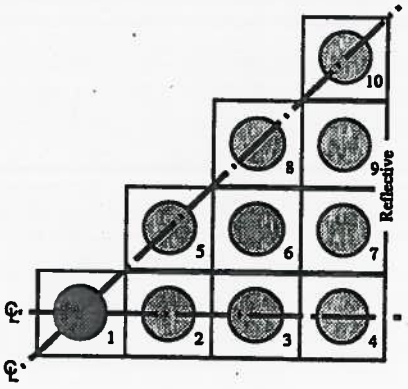


```
$MAC ;
 READ INPUT
 MIX 1 TOTAL  1.250  SCAT 1 1  1.242  FIXE 1.000
 MIX 2 TOTAL  0.625  SCAT 1 1  0.355
 MIX 3 TOTAL 14.000  SCAT 1 1  0.000
 STOP
$GEO ;
 PWR := CAR2D 4 4
     X-  DIAG   X+  REFL
     Y-  SYME   Y+  DIAG
     CELL
           P F F F
             F F F
               F F
                 F ;

     F := CARCEL      1
          RADIUS 0.000 0.450
            MIX       2     1 ;
          MESHX -0.625 0.625
           SPLITX     2
          MESHY -0.625 0.625
           SPLITY     2
     ENDG
     P := F
            MIX       3     1 ;
          SPLITR     3
     ENDG
ENDG
STOP
```

Proceedings of the
International Topical Meeting
Advances in Mathematics, Computations, and Reactor Physics

April 28 - May 2, 1991
Green Tree Marriott, Pittsburgh, PA, USA

Volume 1

Jointly Sponsored by the American Nuclear Society Pittsburgh Section,
Mathematics and Computation Division, and Reactor Physics Division.

Co-sponsored by the Canadian Nuclear Society,
the European Nuclear Society,
and the Atomic Energy Society of Japan.

With the Cooperation
of the Society for Industrial and Applied Mathematics (SIAM).

ISBN: 0-89448-161-4

American Nuclear Society, Inc.
555 North Kensington Avenue
LaGrange Park, IL 60525

Printed in the United States of America
University Graphics and Printing
University of Pittsburgh
April 1991

Cover Design by Matthew Somma